PLOS ONE

RESEARCH ARTICLE

Soleus muscle weakness in cerebral palsy: Muscle architecture revealed with Diffusion Tensor Imaging

Annika S. Sahrmann[1], Ngaire Susan Stott[2], Thor F. Besier[1,3], Justin W. Fernandez[1,3], Geoffrey G. Handsfield[1]*

1 Auckland Bioengineering Institute, University of Auckland, Auckland, New Zealand, **2** Department of Orthopaedic Surgery, Faculty of Medical and Health Sciences, University of Auckland, Auckland, New Zealand, **3** Department of Engineering Science, Faculty of Engineering, University of Auckland, Auckland, New Zealand

* g.handsfield@auckland.ac.nz

Citation: Sahrmann AS, Stott NS, Besier TF, Fernandez JW, Handsfield GG (2019) Soleus muscle weakness in cerebral palsy: Muscle architecture revealed with Diffusion Tensor Imaging. PLoS ONE 14(2): e0205944. https://doi.org/10.1371/journal.pone.0205944

Editor: Christos Papadelis, Boston Children's Hospital / Harvard Medical School, UNITED STATES

Received: September 19, 2018

Accepted: January 24, 2019

Published: February 25, 2019

Data Availability Statement: All soleus masks and fibre vector data are available from Figshare (10.17608/k6.auckland.7672940) and SimTK (https://simtk.org/projects/cpsoleusdti).

Funding: GGH and TFB received funding from the Wishbone Trust of the NZ Orthopaedic Association to pursue this study. [Award Number 3710689; https://nzoa.org.nz/wishbone-orthopaedic-research-foundation-new-zealand; The funder had no role in study design, data collection and

Abstract

Cerebral palsy (CP) is associated with movement disorders and reduced muscle size. This latter phenomenon has been observed by computing muscle volumes from conventional MRI, with most studies reporting significantly reduced volumes in leg muscles. This indicates impaired muscle growth, but without knowing muscle fiber orientation, it is not clear whether muscle growth in CP is impaired in the along-fiber direction (indicating shortened muscles and limited range of motion) or the cross-fiber direction (indicating weak muscles and impaired strength). Using Diffusion Tensor Imaging (DTI) we can determine muscle fiber orientation and construct 3D muscle architectures which can be used to examine both along-fiber length and cross-sectional area. Such an approach has not been undertaken in CP. Here, we use advanced DTI sequences with fast imaging times to capture fiber orientations in the soleus muscle of children with CP and age-matched, able-bodied controls. Cross sectional areas perpendicular to the muscle fiber direction were reduced (37 ± 11%) in children with CP compared to controls, indicating impaired muscle strength. Along-fiber muscle lengths were not different between groups. This study is the first to demonstrate along-fiber and cross-fiber muscle architecture in CP using DTI and implicates impaired cross-sectional muscle growth in children with cerebral palsy.

Introduction

Cerebral Palsy (CP) is one of the most common movement disorders in children. It is a disabling neuromusculoskeletal condition associated with a non-progressive neurological lesion in the brain caused before or during birth or up to two years after birth[1]. Individuals with CP have impaired movements and hypertonia, which can limit both physical activity and social participation[2,3]. Although the neural lesion is non-progressive[4], the biomechanical impairments in CP are progressive, becoming worse as the child grows and ages[5]. Since the progression of CP appears to be musculoskeletal and not neural, this disorder may be greatly illuminated with further investigations into musculoskeletal development in CP.

analysis, decision to publish, or preparation of the manuscript.] GGH received fellowships from the Whitaker Foundation [Award Number N/A; https://www.whitaker.org/] and the Robertson Foundation Aotearoa Fellowship Program [Award Number 3715249; http://robertsonfoundation.org/index.html] during the pursuit of this study. The funders had no role in study design, data collection and analysis, decision to publish, or preparation of the manuscript.

Competing interests: The authors have declared that no competing interests exist.

Previous studies[4,6–11] have reported wide-spread volume deficits of the lower extremity muscles in children with CP when compared to age-matched typically developing (TD) controls. Among these observations, the soleus muscle seems to be especially affected by reduced muscle volume[6]. The soleus is the largest muscle of the triceps surae and plays an essential role in standing and walking[12,13]. Additionally, the soleus appears to act eccentrically during mid-stance to modulate tibial progression; a muscular impairment of the soleus may thus contribute to the excessive knee flexion observed during crouch gait[14]. Alterations in soleus function will thus have profound implications for gait. While muscle volume deficits can be determined relatively easily from medical imaging, these measurements do not indicate whether the muscle is short in the along-fiber direction or small in the cross-fiber direction. Knowledge of muscle fiber orientation can help to understand the nature of reduced volumes in CP. Functionally, muscle area in the cross-fiber direction is related to the muscle's force generating capacity[15,16]. Length of the muscle in the along-fiber direction—fascicle length—is related to the range of motion and contraction velocity of a muscle. To estimate muscle cross-sectional area and fascicle length from medical imaging, we can use specific imaging techniques such as Diffusion Tensor Imaging (DTI) and apply tractography post-processing algorithms. With such knowledge, muscle architecture characteristics such as pennation angle, fascicle length, and cross-section can be calculated to help provide information about functional impairments at the muscle level in children with CP. This information may inform orthopaedic surgeries such as tendon lengthenings, which specifically target a muscle-tendon unit and can be tailored or ruled out with knowledge of the length and cross-sectional area of the muscle being targeted.

One *in vivo* technique for acquiring muscle fiber data is DTI which is a Magnetic Resonance Imaging (MRI) sequence that encodes diffusion to evaluate directions of fluid motion within tissues[17,18]. Since water diffuses preferentially along fibers rather than across them in skeletal muscle, DTI can be used to reconstruct and analyze skeletal muscle fiber tracts[19–23], which can then be used to calculate muscle architecture. The long imaging times of DTI have prevented its use in CP populations in the past, since it is essential that patients remain still for the length of the scanning. Advancements in DTI have made it possible to acquire images quickly, opening up the possibility to use this technology in CP patients.

The purpose of this study was to investigate and compare the muscle fiber architecture of the soleus muscles in children with and without CP, focusing on the along-fiber length, cross-fiber area, and pennation angle. By beginning with a foundational understanding of the muscle architecture in CP and how it differs from TD muscle architecture, the muscular contribution to impaired biomechanics in CP can be illuminated. With muscle fiber architecture, predictions about functional impairments such as reduced strength, fatigue, and impaired gait of children with CP can be more reliable and rehabilitation therapies can be evaluated in terms of muscle architecture.

Materials and methods

Participant characteristics and imaging

Images were collected from 9 volunteers with CP, ranging from level I to III in the Gross Motor Function Classification System[24,25] (GMFCS) with the following characteristics:. [mean ± SD (range)]: age: 11.1 ± 2.0 (8–13) years, height: 145.1 ± 10.8 (125.0–154.0) cm, body mass: 37.7 ± 10.3 (22.0–51) kg, body mass index: 17.6 ± 2.9 (14.1–21.5) kg/m^2. Five participants presented with spastic diplegia, one with spastic hemiplegia, and 3 with non-spastic hemiplegia. Participant characteristics are provided in Table 1. Inclusion criteria included the ability to safely undergo MRI and remain motionless in the MRI scanner for the duration of

Table 1. Characteristics for all CP subjects.

	CP 1	CP 2	CP 3	CP 4	CP 5	CP 6	CP 7	CP 8	CP 9
Age (years)	13	11	12	13	12	8	9	8	8
Gender (M/F)	M	F	F	M	M	M	M	F	F
Height (m)	1.50	1.48	1.54	1.57	1.60	1.25	1.36	1.14	1.17
Weight (kg)	37	31	49	41	51	22	33	17	20
BMI (kg/m^2)	16.4	14.2	20.7	16.6	19.9	14.1	17.8	13.1	14.6
Spasticity?	Yes	Yes	No	Yes	Yes	No	No	Yes	Yes
Hemi/Diplegic	Di	Hemi	Hemi	Di	Di	Hemi	Hemi	Di	Di
GMFCS	II	I	II	III	III	II	I	II	II

https://doi.org/10.1371/journal.pone.0205944.t001

the imaging time. Nine age- and gender-matched typically developed (TD) participants were recruited for comparison as a control group, with the following characteristics: [mean ± SD (range)]: age: 11.1 ± 2.0 (8–13) years, height: 150.6 ± 11.8 (134.0–164.0) cm, body mass: 39.6 ± 8.2 (27.0–51.0) kg, body mass index: 17.3 ± 1.5 (15.0–20.2) kg/m^2. The study protocol was approved by the University of Auckland Human Participants Ethics Committee. Parents/guardians of participants provided informed consent prior to study participation and all participants assented to the study.

Imaging data were collected from knee to ankle. The scanning was conducted on a 3.0T Siemens Skyra Scanner (Erlangen, Germany) using a high-resolution 3D T1 VIBE Dixon sequence with the following parameters: TE/TR: 5.22 ms/ 10.4 ms; FOV: 128mm x 228mm x 384mm [R-L, A-P, S-I]; spatial resolution: 0.8 mm × 0.8 mm × 0.8 mm; imaging time: 5min. After the Dixon scan, we immediately scanned using an echo planar imaging sequence with the following parameters: TE/TR/α: 74.0 ms/ 4400 ms; b-value: 500 mm/s^2; FOV: 200mm x 200mm in-plane; axial slice thickness: 5 mm; in-plane spatial resolution: 1.64 mm × 1.64 mm; two stacks of 35 images; imaging time: 6min. The total scan time for our protocol was just under 20 minutes for the T1 scan and the two DTI scans. The subjects were scanned in feet first supine position with 10˚ of knee flexion. The subjects' ankles were positioned in a neutral orientation using a foam block and pneumatic bean bag. An accessory flex coil and the body coil were used. DTI image stacks were merged with a custom code written in Matlab R2016a (Natick, Massachusetts, USA). Post-processing was conducted using DSI Studio[26].

Image processing

To increase image signal, T1 images were resampled from a slice thickness of 0.8mm to 4mm using Matlab (R2016a). We segmented three characteristic regions of the soleus muscle consistent with regions identified from anatomical studies[27,28] (Fig 1). Segmentation was conducted on T1 images in the axial plane using ITK Snap[29] (V 3.4.0). T1-weighted images were spatially registered to the DT image space and the segmented muscle regions were exported as binary masks for DTI post processing. Fiber tracking was conducted by importing the transformed binary mask into the DSI studio software, and using the fiber tracking algorithm[30] for single-thread DTI implementation with the following parameters: angular threshold: 40˚, fractional anisotropy (FA): $0.1 < FA < 0.5$ (mean 0.31), mean diffisivity (MD): $1{\cdot}10^{-3}mm^2/s < MD < 2{\cdot}10^{-3}mm^2/s$ (mean $1.51{\cdot}10^{-3}mm^2/s$), minimum tract length: 20mm, maximum tract length: 200mm. After this process, DTI tracts were visually inspected to confirm that they originated and terminated near aponeurosis locations. On average, 3900 tracts were extracted per subject. Muscle fascicle lengths were then taken as the DTI tract length.

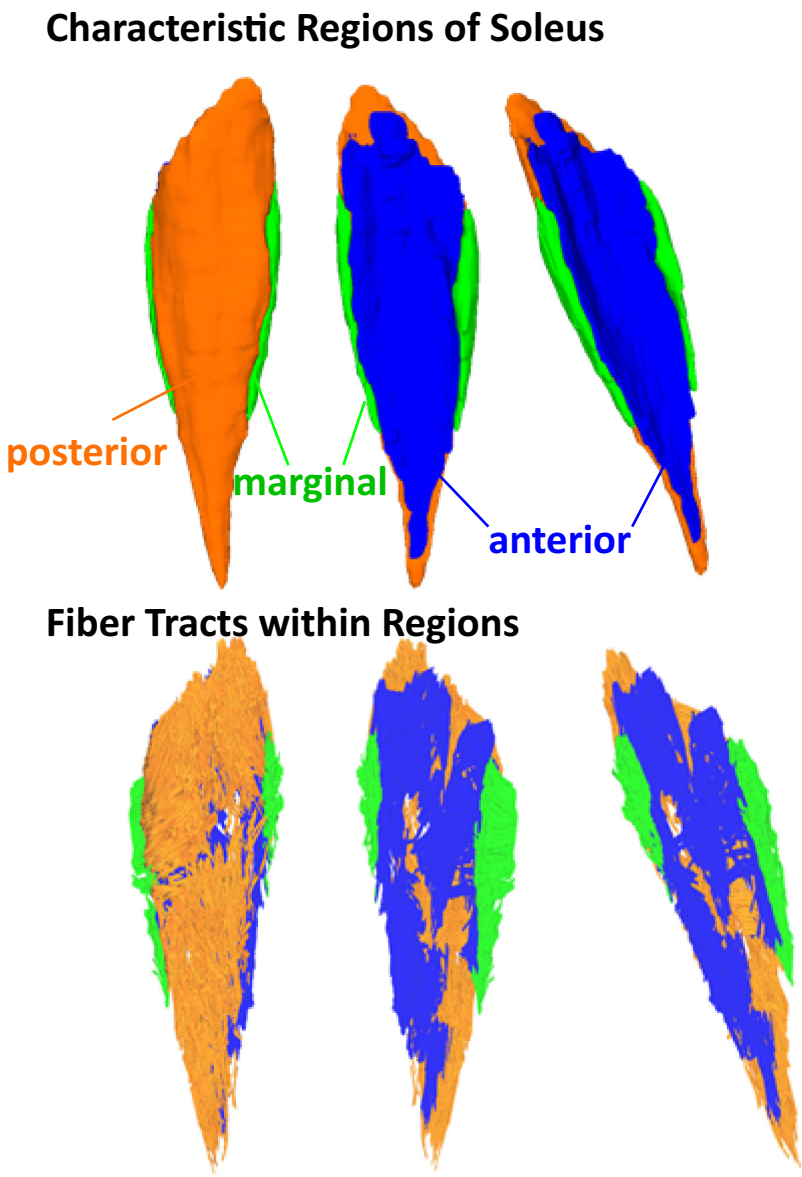

Fig 1. 3D reconstructions of segmented MRI images illustrate the 3 characteristic regions of the soleus muscle—posterior (orange), anterior (blue) and marginal (green). Fiber tracts reconstructed from DTI within those masks represent unique fiber regions within the muscle.

https://doi.org/10.1371/journal.pone.0205944.g001

Muscle cross-sections

PCSA is defined as the cross-sectional area perpendicular to the fiber direction at optimal fiber length[31,32]. In this non-invasive study we were unable to determine sarcomere lengths and PCSA could thus not be computed according to the canonical definition. However, to capture muscle size in the cross-fiber direction, we define CSA_{fib}, a modified CSA according to Eq 1, which is the cross-section of the muscle perpendicular to the fiber directions at the neutral joint angle at which participants were imaged. This parameter differs from PCSA in that it may not represent the cross-section when muscles were at optimal length but differs from CSA in that CSA_{fib} is the area specifically perpendicular to the fiber direction. For each soleus we

calculated CSA_{fib} using:

$$CSA_{fib} = \frac{muscle\ volume}{fascicle\ length} \quad (1)$$

where *muscle volume* is the volume of the soleus acquired from image post-processing in units of cm^2 and fascicle length is the median length of fibers obtained from DTI post-processing in *cm*.

Pennation angle

The conventional definition of pennation angle is the 2D-angle between the muscle fiber and the line of action of the muscle[33,34]. The 2D nature of this definition makes it difficult to apply to complex three dimensional data. Another definition describing 3D angles has been offered in the past[27,35]. Consistent with these, pennation angles were calculated as the angle between the tangent vector of the fiber bundle and the norm vector of the muscle surface at the insertion point of the bundle. Since each region of the muscle consists of multiple differently arranged fiber bundles, one characteristic fiber bundle was extracted for each region and the pennation angle was computed for this fiber bundle for the region from which it was extracted. To have a reasonable comparison of angles, bundles were inspected to ensure consistency of location across subjects.

Normalization and scaling of variables

To reduce the effects of body height and mass on differences in muscle size and architecture, we normalized and scaled computed parameters according to the following equations. Muscle volume was scaled to body size based on findings from a previous study[36]:

$$volume_{scaled} = \frac{muscle\ volume}{height \cdot mass} \quad (2)$$

where *muscle volume* is the volume of the soleus acquired from image processing in units of cm^2, *height-mass* is the product of subject height in *cm* and body mass in *kg*.

CSA_{fib} was scaled to mass:

$$CSA_{fib,scaled} = \frac{CSA_{fib}}{mass} \quad (3)$$

where $CSA_{fib,scaled}$ is in cm^2/kg, CSA_{fib} is the cross-sectional area of the soleus perpendicular to the fiber direction in cm^2 and *mass* is the subject's body mass in *kg*.

Muscle length and fascicle lengths were normalized by height as follows:

$$muscle\ length_{norm} = \frac{muscle\ length}{height} \quad (4)$$

$$fascicle\ length_{norm} = \frac{fascicle\ length}{height} \quad (5)$$

where *muscle length* is the superior-inferior length of the muscle in *cm*, *fascicle length* is the tract length obtained from DTI post-processing in *cm* and *height* is the subject's body height in *cm*.

Statistics

Since normalized parameters were being compared between groups, nonparametric statistical tests were necessary. For all tests of significance, the Wilcoxon ranksum test was used.

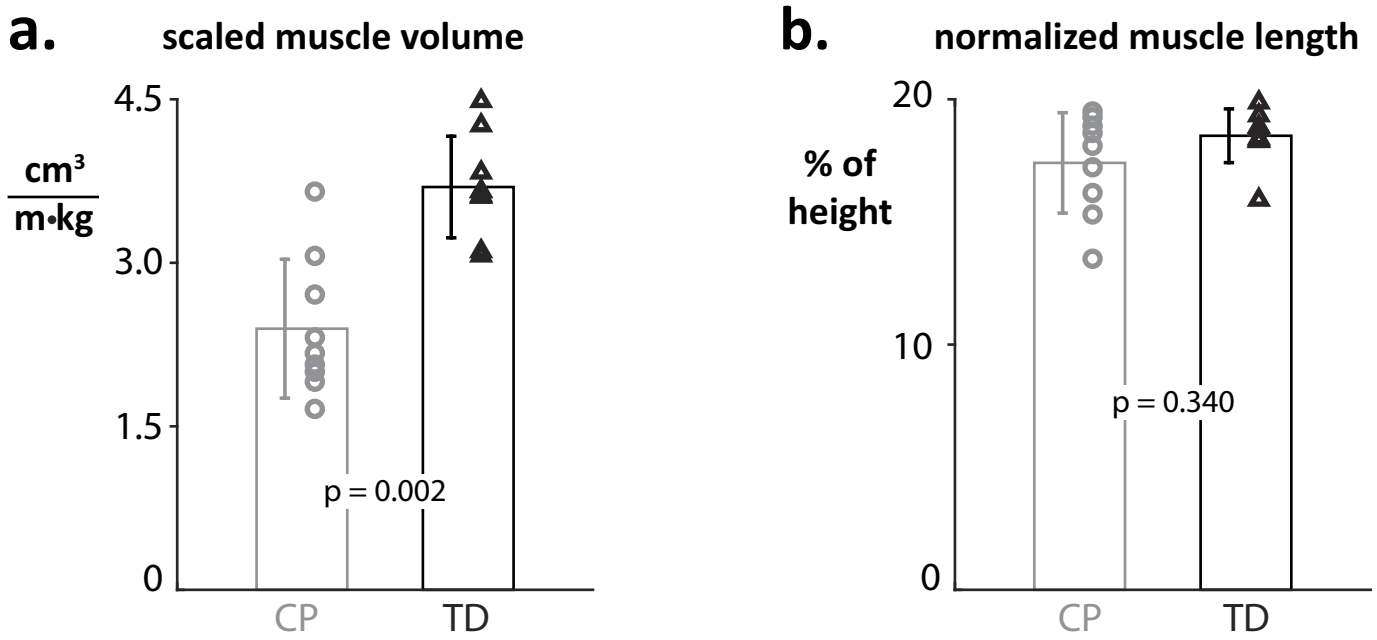

Fig 2. A) Scaled muscle volumes are significantly reduced in the CP cohort. B) Normalized muscle length is longer in the TD population but this difference does not reach significance.

https://doi.org/10.1371/journal.pone.0205944.g002

Results

Muscle volumes and muscle lengths

Muscle volumes differed significantly between the CP and the TD group (Fig 2A). Absolute muscle volumes were 42.6% smaller in the CP group ($p = 0.004$). Body size and mass scaled volumes were 35.2% smaller on average for CP subjects ($p = 0.002$). Differences in muscle length (Fig 2B) did not reach significance for either absolute or normalized lengths: absolute length difference 8.5% ($p = 0.131$), normalized length difference 6.0% ($p = 0.340$).

We observed differences in the shape of the soleus muscle between the CP and TD group and within the CP group. Overall, the fiber models show that CP group has smaller muscles. Also, the subjects with CP show a less dense 'packing' of muscle fibers in their muscles than the subjects of the TD group, suggestive of a larger fraction of intramuscular connective tissue. CP muscles were longer and thinner compared to their TD counterparts.

The CP cohort presented smaller volumes than the TD cohort for each of the three functional regions of the soleus. The marginal region was the most reduced region and was 56.5% smaller in the CP group ($p = 0.001$), the anterior region was 46.1% smaller in the CP group ($p = 0.004$), and the posterior region was 35.5% smaller in the CP group ($p = 0.019$).

Fascicle lengths and CSA_{fib}

A comparison of the median fascicle lengths between the CP and TD groups revealed no significant differences in normalized fascicle length between the cohorts (Fig 3). Absolute fascicle lengths were not significantly different in any compartment between the groups.

We observed heterogeneities in fascicle lengths within both cohorts (Fig 3). For instance, both the longest and the shortest normalized median fascicle length could be found within the TD group (longest 34mm with a height of 1.34m; shortest 24.5mm with a height of 1.36m). Thus, within group heterogeneity was apparent and was also consistent with literature reports

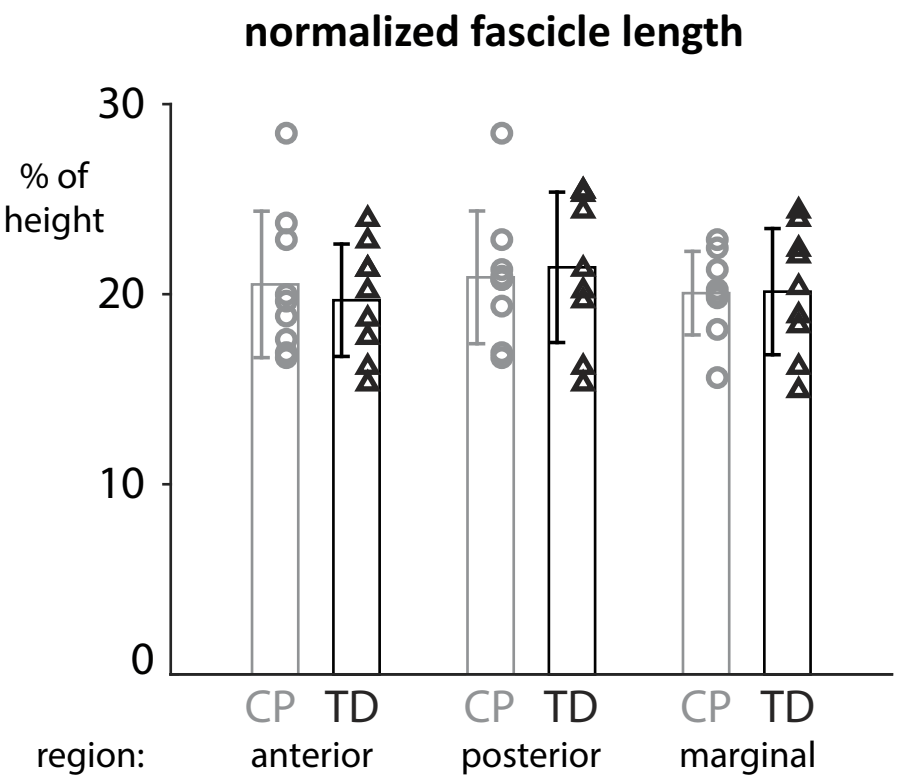

Fig 3. Normalized fascicle lengths in the three regions of the soleus show heterogeneities within and between groups but are not significantly different between CP and TD cohorts.

https://doi.org/10.1371/journal.pone.0205944.g003

of fascicle length heterogeneity (see Discussion). Additionally, we found a large range of fascicle lengths within each subject and muscle compartment. The average standard deviation of fascicle length within a single subject was 7.2mm for the anterior compartment, 6.7mm for the marginal compartment, and 6.3mm for the posterior compartment. While variability was evident within subjects, we did not find any significant differences in fascicle lengths between the CP and TD group.

CSA_{fib} was significantly reduced among the CP cohort: mean deficits of 40.9% in CSA_{fib} ($p = 0.014$) (Fig 4). Mass scaled CSA_{fib} ($CSA_{fib,scaled}$) was reduced by 36.1% in CP subjects ($p = 0.001$). We found no significant differences in CSA_{fib} or $CSA_{fib,scaled}$ between GMFCS levels of the CP cohort. There was a significant correlation between age and CSA_{fib} for the TD cohort ($R2 = 0.923$, $p < 0.0001$) but no significant correlation in the CP group. Correlations between age and $CSA_{fib,scaled}$ were not significant for either group. A direct comparison between each age- and gender-matched subject's CSA_{fib} revealed a smaller CSA_{fib} than their TD counterpart.

Pennation angle

Pennation angle describes how the muscle fibers are arranged and influences muscle function. In this study, we found no significant differences in pennation angle and thus fiber arrangement between the CP and TD cohorts for any of the compartments of the soleus. Computed angles for the selected characteristic fiber bundles varied widely between compartments and also within them (Fig 5). The angular range in the whole muscle ranged from 8.03˚ to 86.9˚. Even within regions ranges were large. In the marginal compartment the pennation angles

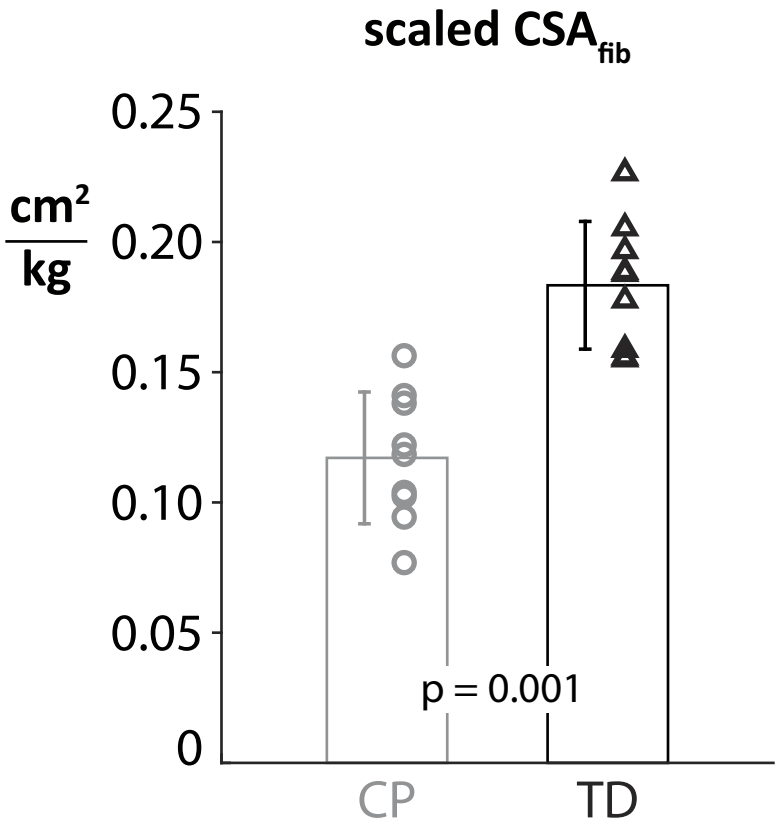

Fig 4. Scaled cross-fiber areas ($CSA_{fib,scaled}$) are significantly reduced in the CP cohort, indicating a reduced maximum force and functional weakness for this muscle. Here, CSA_{fib} was scaled by the body mass of each subject.

https://doi.org/10.1371/journal.pone.0205944.g004

were significantly larger than angles in the anterior and posterior compartments (p = 0.001). Pennation angles were not significantly different between the anterior and posterior compartments.

Discussion

Deficits in muscle volume in CP have been previously observed and reported by many different groups[4,6,8,10,37,38]. In the present study, we also observed significantly reduced muscle volumes. This was true for both absolute and body-size scaled muscle volumes. Deficits in muscle length and fascicle length in CP were not observed. Deficits in cross-fiber areas (CSA_{fib}) in this study were large in the CP group and consistent with literature findings for other lower limb muscles[11,39]. Our results suggest that volume deficits observed in CP are largely related to deficits in cross-section and may indicate impaired strength capacity in CP.

From a geometrical perspective, muscle volume deficits may be related to deficits in fascicle length, PCSA, or both. Functionally, deficits in fascicle lengths may be related to contractures, reduced range of motion, or contraction velocity while deficits in cross-section suggest reduced strength capacities. The findings of the present study suggest that volume deficits in CP are more associated with cross-sectional deficits and implicate decreased strength capacities. Previously reported results on this question are somewhat varied: Handsfield et al.[6] did not determine fascicle lengths but reported reduced muscle lengths of 7.5% in the soleus in CP. Using ultrasound, Shortland et al.[40] and Barber et al.[11] found no fascicle length

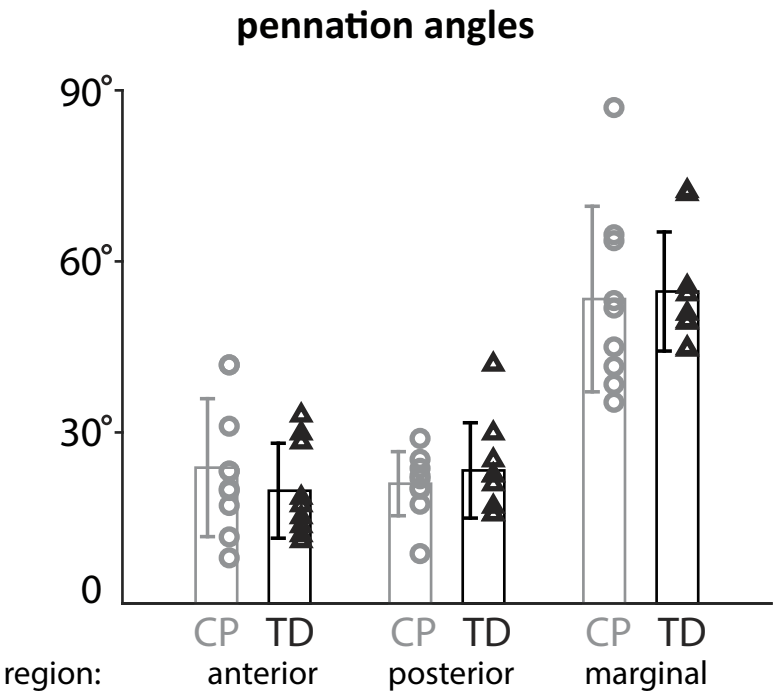

Fig 5. Pennation angles for all subjects in each compartment (marginal, posterior, anterior) show subject-specific results and large angle ranges also within the groups, but no significant differences between the groups.

https://doi.org/10.1371/journal.pone.0205944.g005

differences in the medial gastrocnemius between CP and TD children. Moreau et al.[41] found reduced fascicle lengths in the rectus femoris, but not the vastus lateralis, in CP. Differences between studies may reflect differences in the muscles analyzed and differences between cohorts or may result from methodological differences[19]. The results found here, that fascicle lengths are not significantly different between CP and TD groups, are consistent with previous ultrasound studies of this muscle[42] and with previous reports for other muscles in CP [11,15,40,43]. While DTI has been used in human skeletal muscle with some regularity [19,20,22,23], the applications of DTI to pediatric skeletal muscle are fewer (e.g. 44). The principles of DTI and tractography nevertheless apply to pediatric populations, the main concern being a reduction in signal-to-noise ratio due to movement in the scanner[44], which was minimal in this study due to the short scan times and pneumatic bean bag to hold the limb in position.

It should be noted that sarcomere lengths were unknown in this study. Sarcomere lengths represent a measure of length dependent force generation and passive stiffness and are used to calculate optimal fascicle length[15,45]. Acquisition of sarcomere lengths *in vivo* requires the use of laser diffractometry[42,46] or microendoscopy[47–49], which we did not have access to in this study. In studies using laser diffraction in adolescents with CP, Smith et al.[46] and Mathewson et al. [42] found sarcomere lengths to be about 17–22% longer in spastic hamstrings (gracilis and semitendinosus) muscles and up to 88% longer in the soleus of individuals with equinus contractures undergoing tendon lengthening surgery. A sarcomere length increase of 20% implies a 20% reduction in observed CSA_{fib} at the time of data acquisition. In our study we observed scaled CSA_{fib} deficits of 36%. In light of the potential differences in sarcomere lengths between CP and TD groups, it is possible that CP muscle fibers in our population may have fewer sarcomeres in series that are 'stretched out' to resemble the normal-length fibers in the TD population[15,46]. The effect of overstretched sarcomeres, e.g. in CP, would

be greater passive resistive force within the muscle and reduced ability to generate voluntary active force[42]. Although we did not examine sarcomere lengths in this study, when considered in the context of other studies on CP muscle architecture, it is possible that CP sarcomere lengths are longer than TD, optimal fascicle lengths are shorter than TD, and PCSAs are reduced compared to TD. These results should be interpreted with caution, however, as the manifestation of CP is subject-specific and muscle-specific and there appear to be methodological differences in the results of *in vivo* sarcomere lengths acquired using laser diffraction vs microendoscopy[42,49] Future studies that assess muscle volumes, fascicle lengths, and sarcomere lengths are warranted.

In this study, we found no differences in pennation angle and fiber orientation between CP and TD cohorts. Similar to previous authors, we found variations of pennation angle within the soleus muscle and divided the soleus into functional compartments to help account for some of these variations. In a dissection study, Agur et al.(25) divided the soleus into more than 40 smaller compartments and found considerable angle ranges between compartments, similar to our findings. The orientations Hodgson et al. (26) found in the soleus in a cine PC-MRI study are also similar to our findings (see Fig 6). Hodgson et al. did not have as much information on fiber direction variability since they used velocity encoded MRI to track net tissue motion, rather than fiber directions particularly. These works have illustrated that the soleus has a complex organization comprising three aponeuroses and regions of muscle fibers with varying 3D orientations within and between regions. Fig 6 illustrates a representation of the principal fiber directions projected into the sagittal plane. Fibers are orientated in opposing directions, descending and ascending, on both sides of the anterior aponeurosis. Pennation angle is often regarded as the 2D angle describing the orientation of fibers with respect to the tendon. While useful for certain applications, the 2D definition is a projection into some plane and does not fully account for the complex organization of fibers in 3D space. When considering the full 3D orientations of fibers within the muscle, decomposition into a single 2D angle necessarily discards information. Previous authors who used DTI have computed pennation angle as the minimum angle between an inserting fiber and the plane of the aponeurosis into which it inserts, which is the definition we used in this study. This definition does not assume a singular plane of projection and is simple to compute; however it should be noted that this definition does not describe the azimuthal angular direction off of the aponeurosis in which the fiber is directed. For muscles with complex organizations such as the soleus, consideration should be made in interpreting pennation angles. More broadly, analysis of muscle function in terms of full 3D orientation of fibers may benefit from tools such as a finite element analysis which can account for complex 3D orientations [50,51].

The peak isometric force that a muscle is able to generate is directly related to the PCSA and the specific tension, σ, which is a measure of the force produced per unit area of skeletal muscle. This parameter has been estimated to be between 0.1 and 1.5 MPa[52,53] and is thought to vary somewhat between muscles and between individuals based on fiber type distribution and other factors. While specific tension may then be subject-specific, it is thought to be similar or reduced in subjects with CP compared to TD subjects. Taken together, a reduced PCSA in CP is representative of a direct reduction in peak isometric force. For the present study, isometric strength capacities in our CP cohort are expected to be reduced by an amount related to reported deficits in CSA_{fib}, but may be greater for subjects whose effective specific tension is also reduced.

There are several limitations to this study that bear consideration in addition to those discussed above. In this study, we imaged 9 individuals with cerebral palsy and 9 typically developing controls. This sample size is reasonable for an imaging study where data acquisition is expensive and time consuming; however, a larger population for this study would have

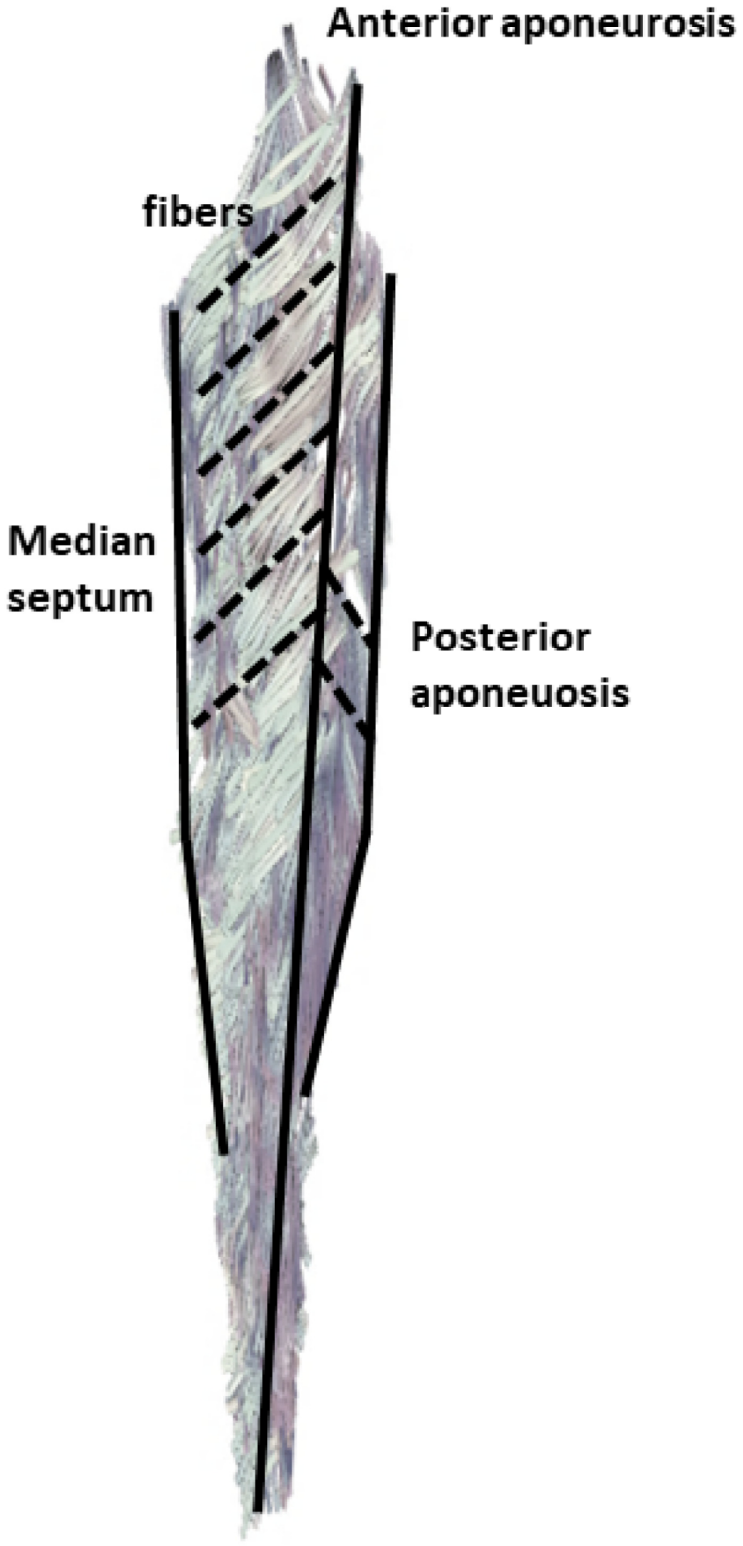

Fig 6. Complex soleus muscle architecture displayed from *in vivo* DTI data, mid-sagittal slice shown. The soleus muscle has three different aponeuroses where fibers originate and insert—the anterior aponeurosis, the median septum, and the posterior aponeurosis. Muscle fibers are oriented in opposite directions on either side of the anterior aponeurosis, creating an inverted "v" appearance.

https://doi.org/10.1371/journal.pone.0205944.g006

conferred greater confidence in our results. As a technique, DTI does not specifically image muscle fibers—rather it is a technique for quantifying diffusion directions of water molecules in the tissue. By filtering the DTI data and implementing tractography algorithms that consider alignment of fibers and overall diffusion directions, muscle fiber tract directions can be reconstructed from DTI. While DTI and correct use of tractography algorithms has been shown to be robust and repeatable in determining muscle fiber directions[21–23,54], the nature of the method requires that users should not view each tract as a *de facto* muscle fiber. Rather the ensemble of tracts represents overall fiber directionality. Given the nature of cerebral palsy, we were unable to guarantee that the muscles of the CP individuals were fully relaxed at time of scan. While none of the subjects were voluntarily contracting their muscles and all of the subjects were in the same ankle and knee angle position with a pneumatic bean bag holding their leg position firmly, spasticity among CP individuals could have caused latent contraction within the muscle even at the same joint angles as the TD counterparts. Future studies using ultrasound, EMG, and microendoscopy may probe this question more fully.

We divided the muscle into three compartments—posterior, anterior, and marginal—to be consistent with literature that investigated the soleus muscle[27,55]. Considering the reconstructed fiber architectures using DTI, it seems possible that it bears defining other compartments as well. The large standard deviations even in small compartments of the soleus also implicate the diversity and complexity even within small spatial regions within the muscle. The large standard deviations we observed are consistent with literature reports where the muscle was divided into 32 compartments and carefully dissected[28]. In these studies, the authors reported large standard deviations within compartments even despite the large number of compartments defined. These results notwithstanding, inspection of fiber directions from DTI in the soleus muscle for our set of subjects reveals that the major fiber orientations appear to be well-described by categorization into the anterior, posterior, and marginal compartments. Further analysis of or definition of alternative compartments may lead to a deeper understanding of this muscle and its function.

In this study, we used DTI and conventional MRI to determine muscle volumes, lengths, and fiber orientations in a CP and a TD population. We compared fascicle lengths and computed CSA_{fib} in the two groups, finding reduced volume and CSA_{fib} in CP. Though we did not compute sarcomere lengths in this study, the magnitude of CSA_{fib} deficits suggest that strength capacity is likely limited in CP due to cross-sectional muscle architecture. Future studies that assess in vivo sarcomere lengths would be a welcome addition as they will determine the magnitude of sarcomere over-stretching at neutral joint angles in CP. Given the complex architecture of the soleus muscle, other tools may prove useful to understanding muscle architecture and its associated function in both cerebral palsy and typically developed populations. Mechanical simulations, for instance, may prove useful to understand how differences in muscle architecture and structure lead to altered function and mechanical behavior[50,51]. An improved understanding of how muscles in CP function may motivate new therapies and help to predict their outcomes. The results of this study implicate muscle strengthening therapies as a potentially effective treatment regime. Physiotherapy, targeted strengthening, and habilitation therapies of muscles in CP may be very beneficial for children and adolescents with CP to strengthen their muscles, improve their muscle function, and improve their quality of life.

Acknowledgments

We wish to acknowledge the contributions of Renee Miller, Beau Pontré, and the helpful staff of the Centre for Advanced MRI, especially Rachel Heron and Anna-Maria Lydon.

Author Contributions

Conceptualization: Ngaire Susan Stott, Thor F. Besier, Justin W. Fernandez, Geoffrey G. Handsfield.

Formal analysis: Annika S. Sahrmann, Geoffrey G. Handsfield.

Funding acquisition: Ngaire Susan Stott, Thor F. Besier, Geoffrey G. Handsfield.

Investigation: Annika S. Sahrmann, Geoffrey G. Handsfield.

Methodology: Annika S. Sahrmann, Ngaire Susan Stott, Thor F. Besier, Justin W. Fernandez, Geoffrey G. Handsfield.

Project administration: Geoffrey G. Handsfield.

Resources: Ngaire Susan Stott, Thor F. Besier, Justin W. Fernandez, Geoffrey G. Handsfield.

Software: Geoffrey G. Handsfield.

Supervision: Ngaire Susan Stott, Thor F. Besier, Justin W. Fernandez, Geoffrey G. Handsfield.

Validation: Geoffrey G. Handsfield.

Visualization: Annika S. Sahrmann, Geoffrey G. Handsfield.

Writing – original draft: Annika S. Sahrmann.

Writing – review & editing: Ngaire Susan Stott, Thor F. Besier, Justin W. Fernandez, Geoffrey G. Handsfield.

References

1. Bax M, Goldstein M, Rosenbaum P, Leviton A, Paneth N, Dan B, et al. Proposed definition and classification of cerebral palsy, April 2005. Dev Med Child Neurol. 2005; 47: 571–576. PMID: 16108461
2. Ko I-H, Kim J-H, Lee B-H. Relationships between lower limb muscle architecture and activities and participation of children with cerebral palsy. J Exerc Rehabil. 2013; 9: 368–374. https://doi.org/10.12965/jer.130045 PMID: 24278886
3. Rosenbaum P, Paneth N, Leviton A, Goldstein M, Bax M, Damiano D, et al. A report: the definition and classification of cerebral palsy April 2006. Dev Med Child Neurol Suppl. 2007; 109: 8–14. PMID: 17370477
4. Oberhofer K, Stott NS, Mithraratne K, Anderson I a. Subject-specific modelling of lower limb muscles in children with cerebral palsy. Clin Biomech. Elsevier Ltd; 2010; 25: 88–94.
5. Morrell DS, Pearson JM, Sauser DD. Progressive Bone and Joint Abnormalities of the Spine and Lower Extremities in Cerebral Palsy. RadioGraphics. 2002; 22: 257–268. https://doi.org/10.1148/radiographics.22.2.g02mr19257 PMID: 11896216
6. Handsfield GG, Meyer CH, Abel MF, Blemker SS. Heterogeneity of muscle sizes in the lower limbs of children with cerebral palsy. Muscle and Nerve. 2016; 53: 933–945. https://doi.org/10.1002/mus.24972 PMID: 26565390
7. Moreau NG, Simpson KN, Teefey SA, Damiano DL. Muscle architecture predicts maximum strength and is related to activity levels in cerebral palsy. Phys Ther. 2010; 90: 1619–1630. https://doi.org/10.2522/ptj.20090377 PMID: 20847035
8. Reid SL, Pitcher CA, Williams SA, Licari MK, Valentine JP, Shipman PJ, et al. Does muscle size matter? The relationship between muscle size and strength in children with cerebral palsy. Disabil Rehabil. 2015; 37(7): 579–84. https://doi.org/10.3109/09638288.2014.935492 PMID: 24989066
9. Noble JJ, Chruscikowski E, Fry NRD, Lewis AP, Gough M, Shortland AP. The relationship between lower limb muscle volume and body mass in ambulant individuals with bilateral cerebral palsy. BMC Neurol. BMC Neurology; 2017; 17: 1–9. https://doi.org/10.1186/s12883-016-0787-9
10. Barrett RS, Lichtwark GA. Gross muscle morphology and structure in spastic cerebral palsy: a systematic review. Dev Med Child Neurol. 2010; 52: 794–804. https://doi.org/10.1111/j.1469-8749.2010.03686.x PMID: 20477832

11. Barber L, Hastings-Ison T, Baker R, Barrett R, Lichtwark G. Medial gastrocnemius muscle volume and fascicle length in children aged 2 to 5years with cerebral palsy. Dev Med Child Neurol. 2011; 53: 543–548. https://doi.org/10.1111/j.1469-8749.2011.03913.x PMID: 21506995
12. Capaday C, Stein RB. Amplitude modulation of the soleus H-reflex in the human during walking and standing. J Neurosci. 1986; 6: 1308–1313. PMID: 3711981
13. Sinkjær T, Andersen JB, Ladouceur M, Christensen LOD, Nielsen JB. Major role for sensory feedback in soleus EMG activity in the stance phase of walking in man. J Physiol. 2000; 523: 817–827. https://doi.org/10.1111/j.1469-7793.2000.00817.x PMID: 10718758
14. Rodda JM, Graham HK, Carson L, Galea MP, Wolfe R. Sagittal gait patterns in spastic diplegia. J Bone Joint Surg Br. 2004; 86–B: 251–258.
15. Lieber RL, Friden J. Functional and clinical significance of skeletal muscle architecture. Muscle Nerve. 2000; 23: 1647–1666. PMID: 11054744
16. Holzbaur KR, Murray WM, Gold GE, Delp SL. Upper limb muscle volumes in adult subjects. J Biomech. 2007; 40: 742–749. https://doi.org/10.1016/j.jbiomech.2006.11.011 PMID: 17241636
17. Jellison BJ, Field AS, Medow J, Lazar M, Salamat MS, Alexander AL. Diffusion Tensor Imaging of Cerebral White Matter: A Pictorial Review of Physics, Fiber Tract Anatomy, and Tumor Imaging Patterns. American Journal of Neuroradiology. 2004; 25(3): 356–369. PMID: 15037456
18. Van Donkelaar CC, Kretzers LJ, Bovendeerd PH, Lataster LM, Nicolay K, Janssen JD, et al. Diffusion tensor imaging in biomechanical studies of skeletal muscle function. J Anat. 1999; 194: 79–88. https://doi.org/10.1046/j.1469-7580.1999.19410079.x PMID: 10227669
19. Bolsterlee B, Veeger HEJ (DirkJan), van der Helm FCT, Gandevia SC, Herbert RD. Comparison of measurements of medial gastrocnemius architectural parameters from ultrasound and diffusion tensor images. J Biomech. Elsevier; 2015; 48: 1133–1140. https://doi.org/10.1016/j.jbiomech.2015.01.012 PMID: 25682540
20. Buck AKW, Ding Z, Elder CP, Towse TF, Damon BM. Anisotropic smoothing improves DT-MRI-based muscle fiber tractography. PLoS One. 2015; 10.
21. Damon BM, Ding Z, Anderson AW, Freyer AS, Gore JC. Validation of diffusion tensor MRI-based muscle fiber tracking. Magn Reson Med. 2002; 48: 97–104. https://doi.org/10.1002/mrm.10198 PMID: 12111936
22. Heemskerk AM, Sinha TK, Wilson KJ, Ding Z, Damon BM. Repeatability of DTI-based skeletal muscle fiber tracking. NMR Biomed. 2010; 23: 294–303. https://doi.org/10.1002/nbm.1463 PMID: 20099372
23. Schenk P, Siebert T, Hiepe P, Güllmar D, Reichenbach JR, Wick C, et al. Determination of three-dimensional muscle architectures: Validation of the DTI-based fiber tractography method by manual digitization. J Anat. 2013; 223: 61–68. https://doi.org/10.1111/joa.12062 PMID: 23678961
24. Palisano R, Rosenbaum P, Walter S, Russell D, Wood E, Galuppi B. Development and reliability of a system to classify gross motor function in children with cerebral palsy. Dev Med Child Neurol. 1997; 39: 214–223. PMID: 9183258
25. Wood E, Rosenbaum P. The gross motor function classification system for cerebral palsy: a study of reliability and stability over time. Dev Med Child Neurol. 2000; 42: 292–296. PMID: 10855648
26. Yeh FC, Verstynen TD, Wang Y, Fernández-Miranda JC, Tseng WYI. Deterministic diffusion fiber tracking improved by quantitative anisotropy. PLoS One. 2013; 8: 1–17.
27. Agur AM, Ng-Thow-Hing V, Ball KA, Fiume E, McKee NH. Documentation and three-dimensional modelling of human soleus muscle architecture. Clin Anat. 2003; 16: 285–293. https://doi.org/10.1002/ca.10112 PMID: 12794910
28. Hodgson JA, Finni T, Lai AM, Edgerton VR, Sinha S. Influence of structure on the tissue dynamics of the human soleus muscle observed in MRI studies during isometric contractions. J Morphol. 2006; 267: 584–601. https://doi.org/10.1002/jmor.10421 PMID: 16453292
29. Yushkevich PA, Piven J, Hazlett HC, Smith RG, Ho S, Gee JC, et al. User-guided 3D active contour segmentation of anatomical structures: Significantly improved efficiency and reliability. Neuroimage. 2006; 31: 1116–1128. https://doi.org/10.1016/j.neuroimage.2006.01.015 PMID: 16545965
30. Jiang H, Van Zijl PCM, Kim J, Pearlson GD, Mori S. DtiStudio: Resource program for diffusion tensor computation and fiber bundle tracking. Comput Methods Programs Biomed. 2006; 81: 106–116. https://doi.org/10.1016/j.cmpb.2005.08.004 PMID: 16413083
31. Alexander RM, Vernon a. The dimensions of knee and ankle muscles and the forces they exert. J Hum Mov Stud. 1975; 1: 115–123.
32. Morse CI. In vivo physiological cross-sectional area and specific force are reduced in the gastrocnemius of elderly men. J Appl Physiol. 2005; 99: 1050–1055. https://doi.org/10.1152/japplphysiol.01186.2004 PMID: 15905324

33. Fukunaga T, Ichinose Y, Ito M, Kawakami Y, Fukashiro S. Determination of fascicle length and pennation in a contracting human muscle in vivo. J Appl Physiol. 1997; 82: 354–358. https://doi.org/10.1152/jappl.1997.82.1.354 PMID: 9029238

34. Narici MM V., Landoni L, Minetti a. EA, M.V. Narici L. Landoni a EM. Assessment of human knee extensor muscles stress from in vivo physiological cross-sectional area and strength measurements. Eur J Appl Physiol. 1992; 65: 438–444.

35. Lansdown DA, Ding Z, Wadington M, Hornberger JL, Damon BM. Quantitative diffusion tensor MRI-based fiber tracking of human skeletal muscle. J Appl Physiol. 2007; 103: 673–681. https://doi.org/10.1152/japplphysiol.00290.2007 PMID: 17446411

36. Handsfield GG, Meyer CH, Hart JM, Abel MF, Blemker SS. Relationships of 35 lower limb muscles to height and body mass quantified using MRI. J Biomech. 2014; 47: 631–8. https://doi.org/10.1016/j.jbiomech.2013.12.002 PMID: 24368144

37. Malaiya R, McNee AE, Fry NR, Eve LC, Gough M, Shortland AP. The morphology of the medial gastrocnemius in typically developing children and children with spastic hemiplegic cerebral palsy. J Electromyogr Kinesiol. 2007; 17: 657–63. https://doi.org/10.1016/j.jelekin.2007.02.009 PMID: 17459729

38. Noble JJ, Fry NR, Lewis AP, Keevil SF, Gough M, Shortland AP. Lower limb muscle volumes in bilateral spastic cerebral palsy. Brain Dev. The Japanese Society of Child Neurology; 2014; 36: 294–300. https://doi.org/10.1016/j.braindev.2013.05.008 PMID: 23790825

39. Barber L, Barrett R, Lichtwark G. Passive muscle mechanical properties of the medial gastrocnemius in young adults with spastic cerebral palsy. J Biomech. Elsevier; 2011; 44: 2496–2500. https://doi.org/10.1016/j.jbiomech.2011.06.008 PMID: 21762920

40. Shortland AP, Harris C a, Gough M, Robinson RO. Architecture of the medial gastrocnemius in children with spastic diplegia. Dev Med Child Neurol. 2002; 44: 158. PMID: 12005316

41. Moreau NG, Teefey S a, Damiano DL. In vivo muscle architecture and size of the rectus femoris and vastus lateralis in children and adolescents with cerebral palsy. Dev Med Child Neurol. 2009; 51: 800–6. https://doi.org/10.1111/j.1469-8749.2009.03307.x PMID: 19459913

42. Mathewson MA, Ward SR, Chambers HG, Lieber RL. High resolution muscle measurements provide insights into equinus contractures in patients with cerebral palsy. J Orthop Res. 2015; 33: 33–39. https://doi.org/10.1002/jor.22728 PMID: 25242618

43. Foran JRH, Steinman S, Barash I, Chambers HG, Lieber RL. Structural and mechanical alterations in spastic skeletal muscle. Dev Med Child Neurol. 2005; 47: 713–717. https://doi.org/10.1017/S0012162205001465 PMID: 16174321

44. Hooijmans MT, Damon BM, Froeling M, Versluis MJ, Burakiewicz J, Verschuuren JJGM, et al. Evaluation of skeletal muscle DTI in patients with duchenne muscular dystrophy. NMR Biomed. 2015; 28: 1589–1597. https://doi.org/10.1002/nbm.3427 PMID: 26449628

45. Ward SR, Eng CM, Smallwood LH, Lieber RL. Are Current Measurements of Lower Extremity Muscle Architecture Accurate? Clin Orthop Relat Res. 2009; 467: 1074–1082. https://doi.org/10.1007/s11999-008-0594-8 PMID: 18972175

46. Smith LR, Lee KS, Ward SR, Chambers HG, Lieber RL. Hamstring contractures in children with spastic cerebral palsy result from a stiffer extracellular matrix and increased in vivo sarcomere length. J Physiol. 2011; 589: 2625–39. https://doi.org/10.1113/jphysiol.2010.203364 PMID: 21486759

47. Cromie MJ, Sanchez GN, Schnitzer MJ, Delp SL. Sarcomere lengths in human extensor carpi radialis brevis measured by microendoscopy. Muscle Nerve. 2013; 48: 286–92. https://doi.org/10.1002/mus.23760 PMID: 23813625

48. Llewellyn ME, Barretto RPJ, Delp SL, Schnitzer MJ. Minimally invasive high-speed imaging of sarcomere contractile dynamics in mice and humans. Nature. 2008; 454: 784–8. https://doi.org/10.1038/nature07104 PMID: 18600262

49. Chen X, Delp SL. Human soleus sarcomere lengths measured using in vivo microendoscopy at two ankle flexion angles. J Biomech. Elsevier; 2016; 49: 4164–4167. https://doi.org/10.1016/j.jbiomech.2016.11.010 PMID: 27866676

50. Alipour M, Mithraratne K, Fernandez J. A diffusion-weighted imaging informed continuum model of the rabbit triceps surae complex. Biomech Model Mechanobiol. 2017; 16: 1729–1741. https://doi.org/10.1007/s10237-017-0916-4 PMID: 28516387

51. Fernandez J, Mithraratne K, Alipour M, Handsfield G, Besier T, Zhang J. Rapid Prediction of Personalised Muscle Mechanics: Integration with Diffusion Tensor Imaging. Imaging for Patient-Customized Simulations and Systems for Point-of-Care Ultrasound; 2017. 71–77.

52. Arkin AM. Absolute Muscle Power: The Internal Kinesiology of Muscle. Arch Surg. 1941; 42: 395–410.

53. Pruim GJ, de Jongh HJ, ten Bosch JJ. Forces acting on the mandible during bilateral static bite at different bite force levels. J Biomech. 1980; 13: 755–763. PMID: 7440590

54. Handsfield GG, Bolsterlee B, Inouye JM, Herbert RD, Besier TF, Fernandez JW. Determining skeletal muscle architecture with Laplacian simulations: a comparison with diffusion tensor imaging. Biomech Model Mechanobiol. 2017; 16: 1–11.

55. Sinha U, Sinha S, Hodgson J a, Edgerton R V. Human soleus muscle architecture at different ankle joint angles from magnetic resonance diffusion tensor imaging. J Appl Physiol. 2011; 110: 807–819. https://doi.org/10.1152/japplphysiol.00923.2010 PMID: 21164150